Supporting Information for

Dual Modality Optical/PET imaging of PARP1 in Glioblastoma

Journal: Molecular Imaging and Biology

Giuseppe Carlucci[1, ‡], Brandon Carney[1, 2, 3, ‡], Christian Brand[1], Susanne Kossatz[1], Christopher P. Irwin[1], Sean D. Carlin[1], Edmund J. Keliher[4], Wolfgang Weber[1, 5], & Thomas Reiner[1, 5 *]

[1] Department of Radiology, Memorial Sloan Kettering Cancer Center, New York, New York 10065, United States

[2] Department of Chemistry and Biochemistry, Hunter College of the City University of New York, New York, New York 10065, United States

[3] Ph.D. Program in Chemistry, The Graduate Center of the City University of New York, New York 10018, United States

[4] Center for Systems Biology, Massachusetts General Hospital, Boston, Massachusetts 02114, United States

[5] Weill Cornell Medical College, New York, New York 10065, United States

Table of Contents

EXPERIMENTAL SECTION

Materials. Commercially available compounds were used without further purification unless otherwise stated. Tetrabutylammonium bicarbonate (TBAB, 0.075 M in water) was purchased from ABX advanced biochemical compounds GmbH (Radeberg, Germany). Extra dry acetonitrile (MeCN) over molecular sieves was purchased from Acros Organics (Geel, Belgium). Water (>18.2 MΩcm^{-1} at 25 °C) was obtained from an Alpha-Q Ultrapure water system from Millipore (Bedford, MA). Tin(IV) chloride ($SnCl_4$, 1 M in methylene chloride) was purchased from Sigma Aldrich (St. Louis, MO). BODIPY-FL succinimidyl ester was purchased from Life Technologies (Carlsbad, CA). (AZD2281) was purchased from LC Laboratories (Woburn, MA). PARPi-FL was synthesized as described earlier [1]. No-carrier-added (n.c.a.) [^{18}F]fluoride was obtained via the ^{18}O(p,n)^{18}F nuclear reaction of 11-MeV protons in an EBCO TR-19/9 cyclotron using enriched ^{18}O-water. QMA light ion-exchange cartridges and C-18 light Sep-Pak® cartridges were obtained from Waters (Milford, MA). High performance liquid chromatography (HPLC) purification and analysis was performed on a Shimadzu UFLC HPLC system equipped with a DGU-20A degasser, a SPD- M20A UV detector, a RF-20Axs fluorescence detector, a LC-20AB pump system, and a CBM-20A communication BUS module. A LabLogic Scan-RAM radio-TLC/HPLC-detector was used for purifications while a PosiRAM Model 4 was used for analysis. HPLC solvents (Buffer A: 0.1% TFA in water, Buffer B: 0.1% TFA in MeCN) were filtered before use. HPLC purification and analysis was performed on a reversed phase Atlantis T3 column (C18, 5 μm, 4.6 mm × 250 mm; flowrate: 0.8 ml/min; gradient: 0-17 min 30-90% B; 17-24 min 90% B; 24-28.5 min 90%-30% B; 28.5-30 min 30% B).

Electrospray ionization mass spectrometry (ESI-MS) spectra were recorded with a Shimadzu LC-2020 with electrospray ionization SQ detector. All PET imaging experiments were conducted on a microPET INVEON camera equipped with a CT scanner (Siemens, Knoxville, TN). Digital phosphor autoradiography of histological U87

MG tumors, muscle and brain were obtained using a Typhoon FLA 7000 laser scanner from GE Healthcare (Port Washington, NY).

Cell culture

The human glioblastoma cell lines U87 MG were kindly provided by Dr. Ronald Blasberg (MSKCC, New York, NY). Cell lines were grown in Eagle's Minimal Essential Medium (MEM), 10% (vol/vol) heat inactivated fetal bovine serum, 100 IU penicillin, and 100 μg/mL streptomycin, purchased from the culture media preparation facility at MSKCC (New York, NY).

Mouse models

All animal experiments were done in accordance with protocols approved by the Institutional Animal Care and Use Committee of MSKCC and followed National Institutes of Health guidelines for animal welfare. Female athymic nude CrTac:NCr-Foxn1^{nu} mice at age 6 - 8 weeks were purchased from Taconic Laboratories (Hudson, NY). Non tumor-bearing mice used to determine the blood half-life of PARPi-FL (n = 4). Xenograft mouse models were used to determine the pharmacokinetics (n = 20). For subcutaneous injections, mice were anesthetized with 2% isoflurane (Baxter Healthcare) (2 l/min medical air). U87 MG cells were implanted subcutaneously (5×10^6 cells in 200 μl 1:1 PBS/matrigel® (BD Biosciences, San Jose, CA) in the right shoulder and allowed to grow for approximately two weeks until the tumors reached 5–10 mm in size. For all intravenous injections, mice were gently warmed with a heat lamp and placed on a restrainer. The tails were sterilized with alcohol pads, and injection took place via the lateral tail vein.

PARP1 Immunohistochemistry

Immunohistochemical staining of PARP1 (Fig. S4) was performed with formalin-fixed, paraffin-embedded U87 MG xenografts and mouse brain using the Discovery XT processor (Ventana Medical Systems, Tucson, AZ) at the Molecular Cytology Core Facility of MSKCC. Following deparaffinization with EZPrep buffer and antigen retrieval with CC1 buffer (both Ventana Medical Systems), sections were blocked for 30

min with Background Buster solution (Innovex, Lincoln, RI). Primary rabbit anti-PARP1 antibody (sc-7150, 0.4 μg/ml, Santa Cruz, Dallas, TX) was incubated for 5 h followed by a biotinylated goat anti-rabbit IgG for 1 h (PK6101, 1:200 Vector labs, Burlingame, CA). Signal detection was performed with a DAB detection kit (Ventana Medical Systems, Tucson, AZ) according to the manufacturers instructions. Sections were counterstained with hematoxylin and coverslipped with Permount (Fisher Scientific, Waltham, MA). Adjacent sections were stained with Hematoxylin and Eosin for morphological evaluation of the tissue.

Radiosynthesis of [^{18}F]PARPi-FL

In a typical experiment, the [^{18}F]fluoride in water was transferred into a sealed conical drying vessel containing TBAB (75 mM in water, 80 μl, 1.8 mg, 6.0 μmol). Water was removed from the [^{18}F]F$^-$/TBAB solution by azeotropic distillation with dry acetonitrile (3 × 1 ml) under a gentle stream of nitrogen at 110 °C. The dry residue was reconstituted with 100 μl of MeCN and cooled to room temperature. To this, PARPi-FL (50 μg, 0.78 μmol) in MeCN (50 μl) was added, followed by 10 equivalents of $SnCl_4$ (100 mM in acetonitrile, 7.8 μmol). The mixture was then heated at 35 °C for 30 min. After incubation, the reaction mixture was cooled to room temperature and diluted with ultrapure water to reach a final 20% MeCN concentration. The crude mixture was filtered with PES 0.22 μm 30 mm diameter (Shirley, MA) and automatically injected into the HPLC system (gradient A) for purification. The [^{18}F]PARPi-FL peak was collected (rt: 17.5 min) and the solution passed through a C18 light-SepPak® cartridge (preconditioned with EtOH (5 ml) and water (5 ml). The cartridge was washed with water (3 ml) and [^{18}F]PARPi-FL was eluted using EtOH (1 ml). The organic solvent was removed by rotary evaporation at 40 °C and the residual product formulated in 15% PEG300 in 0.9% saline for *in vivo* animal imaging and biodistribution. The labeling procedure was fully automated using a ScanSys radiochemistry module from ScanSys (Vaerloeser, Denmark).

Small-animal PET imaging

Mice bearing subcutaneous U87 MG (n = 12) were divided in two groups (non blocked and blocked) and administered with [^{18}F]PARPi-FL [200 μCi, 160 mCi/μmol) in 200 μl

15% PEG300 in 0.9% sterile saline] via tail vein injection. Approximately 5 min prior to PET acquisition, mice were anesthetized by inhalation of a mixture of isoflurane (Baxter Healthcare, Deerfield, IL, USA; 2% isoflurane, 2 l/min medical air) and positioned on the scanner bed. Anesthesia was maintained using a 1% isoflurane/O_2 mixture. PET data for each mouse was recorded using static scans of 30 minutes and acquired at 1 h post-injection. The blocked cohort (n = 6) was pre-injected with the PARP1 inhibitor olaparib (500 mM, 3.7 μmol, in 100 μl 15% PEG300 / 85% 0.9% saline). Images were analyzed using INVEON software (Siemens, Knoxville, TN). Quantification and %ID/g values were calculated by manually drawing regions of interests in four different frames and calculating the average values. Standard Uptake Values (SUV) were calculated for 3D regions of interest (ROI), using Inveon Research Workplace software (Siemens Medical Solutions, Knoxville, TX). Tumor ROIs drawn on the images, normalized to the injected dose and body weight and converted to SUV.

Ex vivo biodistribution

Biodistribution studies were performed in U87 MG xenografted athymic nude mice (n = 4). Mice were divided in two groups (positive controls and blocked) and administered with [^{18}F]PARPi-FL [approximately 27 μCi, 160 mCi/μmol) in 200 μl, 15% PEG300 in 0.9% sterile saline] via tail vein injection. The blocked group was pre-injected with an excess of Olaparib (500 mM, 3.7 μmol, in 100 μl 15% PEG300 / 85% 0.9% saline). Mice were sacrificed by CO_2 asphyxiation at 90 min p.i. and major organs were collected, weighed, and counted in a WIZARD^2 automatic γ-counter (PerkinElmer, Boston, MA). The radiopharmaceutical uptake was expressed as a percentage of injected dose per gram (%ID/g) using the following formula: [(activity in the target organ/grams of tissue)/injected dose]×100%.

Blood half-Life

The blood half-life of [^{18}F]PARPi-FL was calculated by measuring the activity of blood samples collected at different time points p.i. (5, 15, 30, 60, and 120 min). Female nude mice (n = 4) were injected via lateral tail vein with [^{18}F]PARPi-FL (50 μCi in 200 μl 15%

PEG300 in 0.9% sterile saline) and blood samples were collected from the great saphenous vein of each animal at the predetermined time point. The collected blood was weighed and counted in a WIZARD^2 automatic γ-counter (PerkinElmer, Boston, MA). The blood half-life was calculated using Prism 6.0c (GraphPad Software, La Jolla, CA) using a two-phase decay least squares fitting method and expressed as %ID/g.

Autoradiography and Hematoxylin–Eosin staining

The collected organs were flash-frozen in liquid Nitrogen and fixed in Tissue-Tek O.C.T. compound (Sakura Finetek, Torrance, CA) and cut into 10 μm sections using a Vibratome UltraPro 5000 Cryostat (Vibratome, St. Louis, MO). A storage phosphor autoradiography plate (Fujifilm, BAS-MS2325, Fiji Photo Film, Japan) was exposed to the tissue slices overnight at -20 °C and read the following day. Relative count intensity of the sections in each image was quantified using ImageJ 1.47u processing software (source: http://rsbweb.nih.gov/ij/) [2]. Tumor/muscle and brain/muscle ratios were calculated using Prism 6.0c (GraphPad Software, La Jolla, CA). The same sections were subsequently subjected to H&E staining (hematoxylin–eosin) for white light microscopy.

Surface fluorescence imaging

While the cellular pharmacokinetics [1, 3, 4] and macroscopic/organ-specific distribution [5] of PARPi-FL have been reported in the past, the possibility of bimodal optical/PET imaging with [^{18}F]PARPi-FL has not been described. For this, U87 MG tumor bearing mice (n = 12) were injected with [^{18}F]PARPi-FL [approximately 27 μCi, 160 mCi/μmol in 200 μL 15% PEG300 in 0.9% sterile saline] via tail vein injection. After PET imaging, the mice were sacrificed and tumor, brain, and muscle harvested, placed on a petri dish and imaged with an IVIS Spectrum fluorescence imaging system (PerkinElmer, Boston, MA) and Living Image 4.4 software. As a negative control group, U87 MG tumor bearing mice (n = 4) were injected with vehicle only (200 μl 15% PEG300 in 0.9% sterile saline). For blocking studies, U87 MG cells were implanted and grown in mice as stated above. The mice were injected with [^{18}F]PARPi-FL as stated above, with the exception that they were injected with an excess Olaparib in 100 μl of 15% PEG300 in 0.9% sterile saline prior to injection of [^{18}F]PARPi-FL. Image analysis for the [^{18}F]PARPi-FL uptake

and blocking study was performed by drawing regions of interest through each organ to calculate the cross-section fluorescence with ImageJ 1.47u image processing software.

Statistical analysis

All data are expressed as mean ± SD. Differences between mouse cohorts were analyzed with the 2-sided unpaired Student test and were considered statistically significant when $P < 0.05$.

SUPPLEMENTARY FIGURES AND TABLES

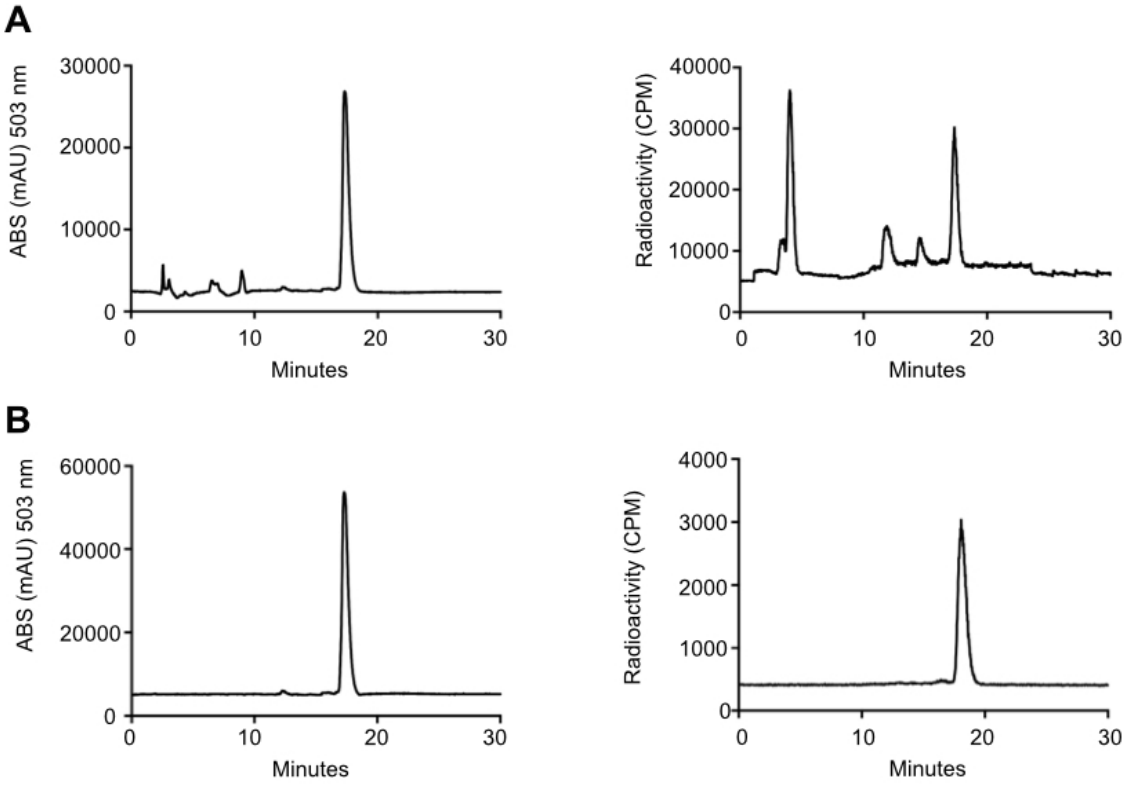

Figure S1: Analytical HPLC chromatograms.

(A) Analytical HPLC trace of absorbance (left) and radioactivity (right) for the crude reaction mixture before semi-prep HPLC purification; (B) Analytical HPLC trace of absorbance (left) and radioactivity (right) for [^{18}F]PARPi-FL following purification and formulation in 15% PEG (75% saline).

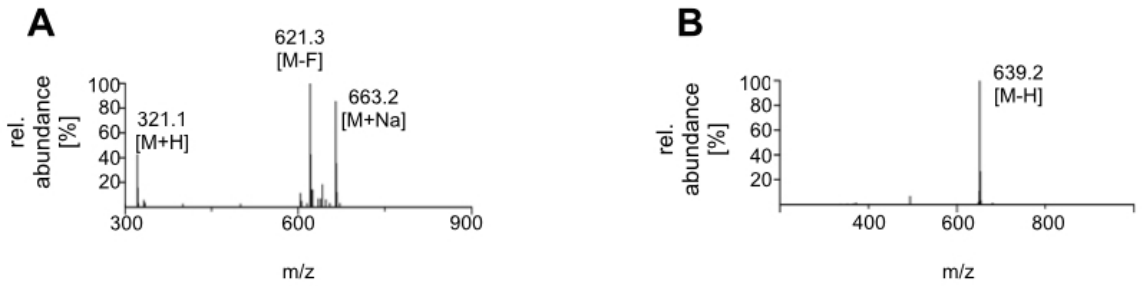

Figure S2: Mass spectrometry characterization data.

(A) Positive polarity ESI-MS and (B) negative polarity ESI-MS spectra of synthesized [^{18}F]PARPi-FL in acetonitrile (70%) / water (30%).

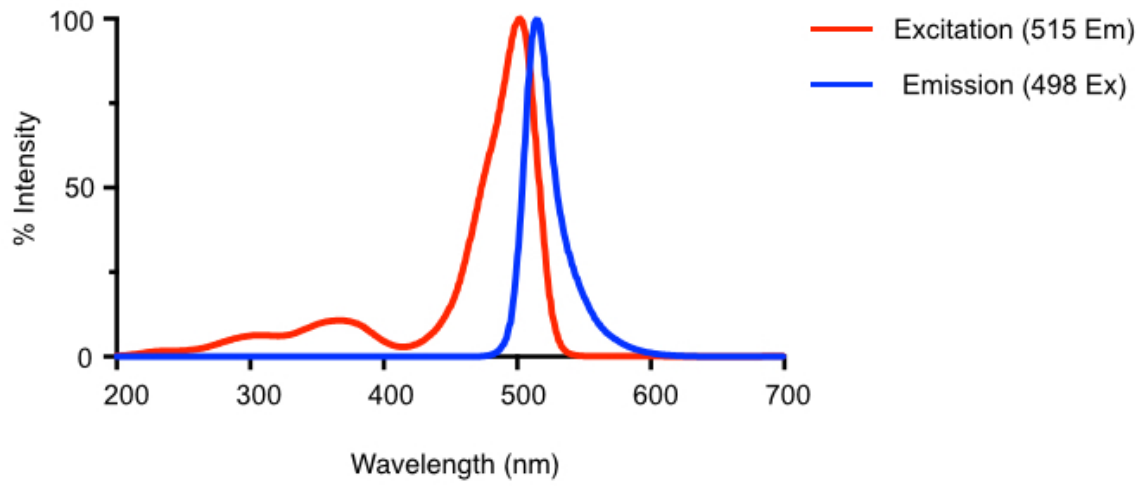

Figure S3: [^{18}F]PARPi-FL fluorescence and emission spectra.

Synthesized [^{18}F]PARPi-FL was injected onto a HPLC equipped with a fluorescence detector and excitation/emission spectra recorded. Excitation spectrum collected at 515nm, emission spectrum excited at 498nm.

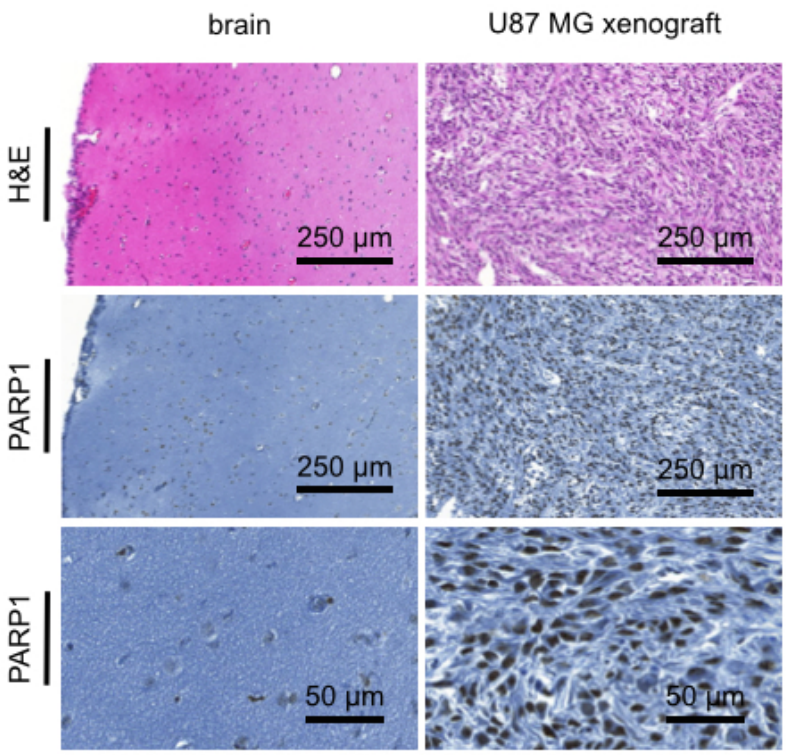

Figure S4: H&E and PARP1 staining of U87 MG xenografts and brain tissues. PARP1 expression in normal mouse brain (left column) and U87 MG xenograft tissue (right column). Morphological aspects are shown in H&E staining (top panel). PARP1 staining in adjacent sections is shown in low (middle panel) and high magnification (bottom panel).

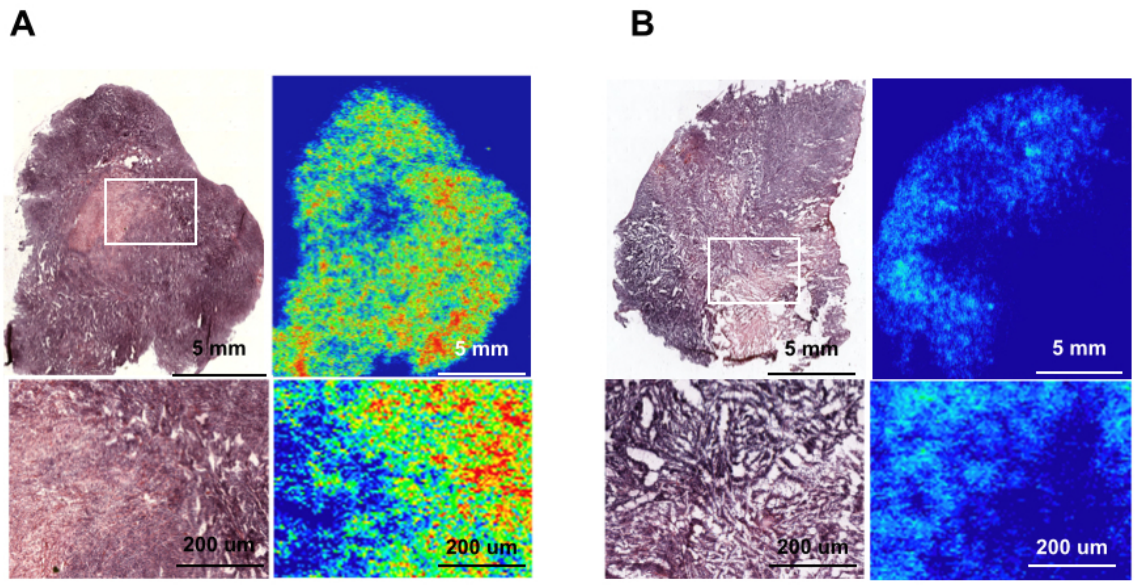

Figure S5: H&E staining and ex vivo autoradiography of U87 MG xenografts.

10 μm sections of resected tissues (U87 MG tumor) were obtained from mice at 90 min p.i. of (A) 200 μCi of [^{18}F]PARPi-FL and (B) both Olaparib (excess injected as blocking agent 30 min before) and 200 μCi of [^{18}F]PARPi-FL. H&E staining correlates with the retention of radioactive material. Bottom panels indicate the expansion of squared defined area where necrotic tissue is observed.

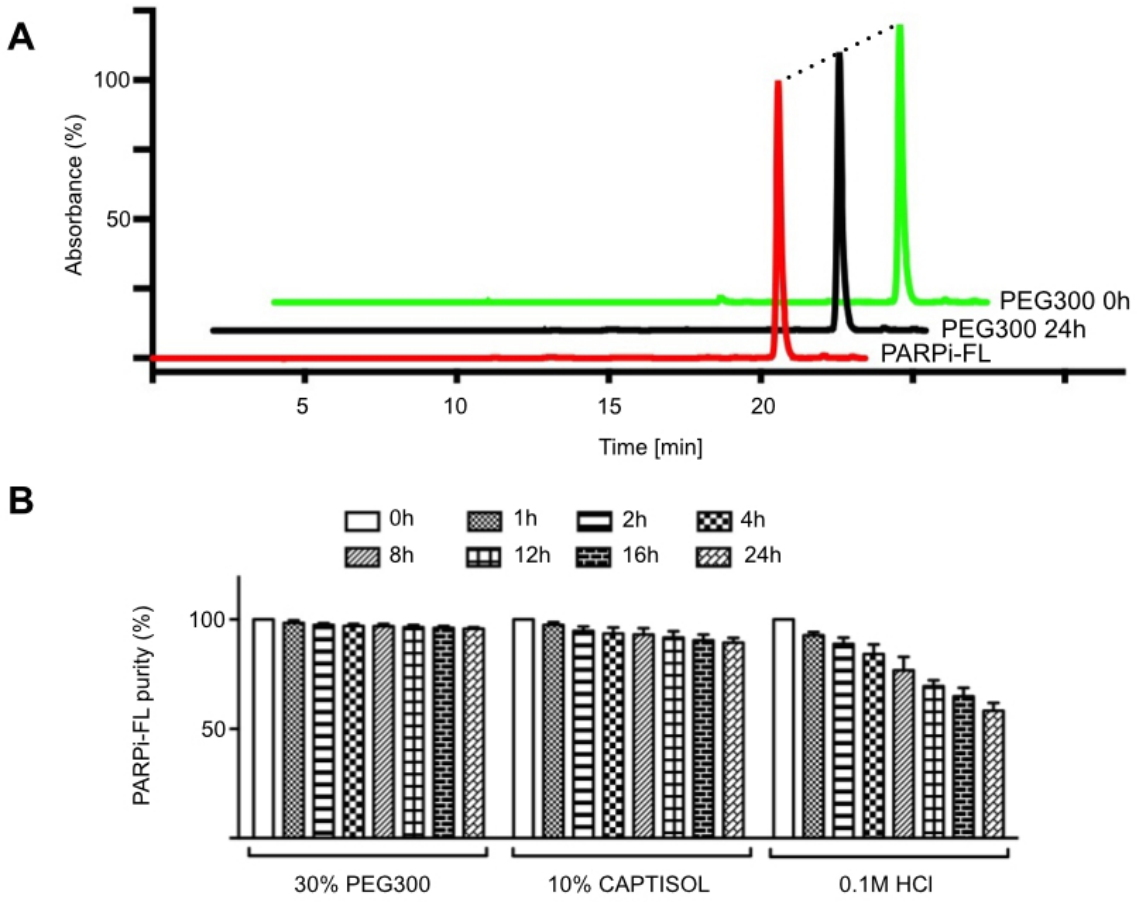

Figure S6: PARPi-FL stability and formulation.

(A) Stability of ^{19}F-PARPi-FL was checked by HPLC equipped with an Atlantis T3 column (C18, 5 μm, 4.6 mm × 250 mm; flow rate: 0.8 mL/min; gradient: 0-17 min 30-90% B; 17-24 min 9% B; 24-28.5 min 90%-30% B; 28.5-30 min 30% B) after formulation in 30% PEG300 (70% PBS). Chromatograms were acquired at 0 minutes and 24 hours after formulation and compared with ^{19}F-PARPi-FL QC. (B) 30% PEG300, 10% Captisol and 0.1M HCl were tested as formulations for PARPi-FL. HPLC chromatograms were obtained at different time points (0, 1, 2, 4, 8, 12, 16, 24 h respectively) and PARPi-FL fraction collected and plotted as % of the area of pure compound. (n=4) $P < 0.05$.

Production type	Radiochemical Yield [%]	Radiochemical Purity [%]	Specific Activity [mCi/µmol]	Total Reaction Time
Non-Automated	23 ± 8.2	85	3	90 min
Automated Module	30.3 ± 7.3	>95	8	70 min

Table S1: Comparison of non-automated to automated [^{18}F]PARPi-FL radiosynthesis.

Same conditions (50 µg PARPi-FL precursor, 10 mCi n.c.a. ^{18}F-, 30 minutes incubation, 35 °C, 10 eq. $SnCl_4$, 0.2 ml reaction volume) were tested for both a non-automated and automated synthesis (n = 6).

	Non Blocked		Blocked	
Organ	% ID/g	SD	% ID/g	SD
Tumor	0.78	0.10	0.15	0.06
heart	0.23	0.04	0.21	0.11
lung	0.42	0.13	0.41	0.20
blood	0.41	0.21	1.02	0.38
liver	3.79	0.43	2.32	0.64
spleen	3.31	0.27	1.38	1.31
pancreas	0.61	0.14	0.27	0.18
kidney	0.76	0.15	0.49	0.17
small intestine	1.70	1.10	3.16	2.90
large intestine	2.19	3.50	0.34	0.18
stomach	0.42	0.21	0.43	0.19
bone	12.07	5.93	13.47	4.24
muscle	0.19	0.05	0.24	0.08
brain	0.06	0.005	0.08	0.016

Table S2: Biodistribution.

Biodistribution of [^{18}F]PARPi-FL in U87 MG xenograft mouse models sacrificed at 90 min time point. Effects of blocking were observed after injection of an excess of

Olaparib (n = 4 per group). 200 μCi / 0.2 ml / each mouse. Values are plotted as %ID/g. SD represents standard deviation.

REFERENCES

1. Reiner T, Lacy J, Keliher EJ, et al. (2012) Imaging therapeutic PARP inhibition in vivo through bioorthogonally developed companion imaging agents. Neoplasia 14:169-177.
2. Schneider CA, Rasband WS, Eliceiri KW (2012) NIH Image to ImageJ: 25 years of image analysis. Nat Meth 9:671-675.
3. Thurber GM, Yang KS, Reiner T, et al. (2013) Single-cell and subcellular pharmacokinetic imaging allows insight into drug action in vivo. Nat Commun 4:1504.
4. Thurber GM, Reiner T, Yang KS, Kohler RH, Weissleder R (2014) Effect of Small-Molecule Modification on Single-Cell Pharmacokinetics of PARP Inhibitors. Mol Cancer Ther 13:986-995.
5. Irwin CP, Portorreal Y, Brand C, et al. (2014) PARPi-FL - a Fluorescent PARP1 Inhibitor for Glioblastoma Imaging. Neoplasia 16:432-440.